ISSN 1063-7710, Acoustical Physics, 2018, Vol. 64, No. 6, pp. 789–795. © Pleiades Publishing, Ltd., 2018.

ACOUSTIC SIGNAL PROCESSING AND COMPUTER SIMULATION

Study on the Mechanism of Ultrasonic Power Measurement Sensor based on Pyroelectric Effect[1]

Yonggang Cao[a], *, Qian Chen[a], Huifeng Zheng[a], Lidong Lu[a], Yuebing Wang[a], and Jiang Zhu[b], **

[a] *College of Metrology and Measurement Engineering, China Jiliang University, Hangzhou, 310018 China*

[b] *Department of Diagnostic Ultrasound, Sir Run Run Shaw Hospital, Zhejiang University College of Medicine, Hangzhou, 310016 China*

**e-mail: 15A0202111@cjlu.edu.cn*

***e-mail: zhujiang1046@zju.edu.cn*

Received December 7, 2017

Abstract—PVDF pyroelectric sensor has been widely applied in many fields, such as intruder alarm. Nowadays, this sensor shows a potential for ultrasonic power measurement. However, the transformation mechanism between the acoustic and pyroelectric signals has not been particularly studied until now. In this paper, a physical model was introduced for theoretical study of the mechanism of energy transformations. In addition, a simulation program based on finite-element analysis method was built up for analyzing the ultrasound propagation characteristics and the temperature rise on the PVDF, as well it predicted the waveform and amplitude of the generated pyroelectric signal. Besides that, a PVDF pyroelectric sensor was fabricated and used for acoustic power measurement experiment. Finally, the experiment and simulation results were compared, confirming that the physical model is suitable for pyroelectric sensor characteristics analysis. It can also provide useful suggestions for the design and fabrication of PVDF pyroelectric sensors with high sensitivity.

Keywords: PVDF, pyroelectric sensor, ultrasonic power, finite-element analysis

DOI: 10.1134/S1063771018060015

INTRODUCTION

The pyroelectric effect, whereby a temperature change in polarity materials will cause the release of the electric charge, was described by Theophrastus in 315 BC. However, it is only since about the 19th century that the applications of pyroelectric effect have been gradually increased. The effect occurs in many materials (single crystals and ceramics) [1]. Studies show that a single crystal provides high Curie temperature, but the pyroelectric coefficient is small. The preparation technology of ceramics is simple and low-cost, but it is hard to get the spontaneous polarization film [2]. In 1960s, another kind of pyroelectric polymer, Polyvinylidene fluoride (PVDF), was put forward. As a polymer, it could be fabricated into a polymer pyroelectric sensor with any size and shape.

Besides the above advantages, the PVDF pyroelectric sensor also has other features, such as fast response, high sensitivity, convenience, etc. Therefore, these sensors have been widely applied in many fields. Based on PVDF pyroelectric effect, Wang [3] made an energy acquisition system, which could improve the energy acquisition and storage. Wang [4] designed a PVDF pyroelectric sensor, which was applied in the infrared detection and automatic switch. Recently, this sensor has been used for acoustic application. Especially, the acoustic power is the main energy characteristic used in the calibration of the ultrasonic instrument [5]. Zeqiri [6, 7] designed a novel PVDF pyroelectric sensor for measuring ultrasonic transducer output power, and studied the pyroelectric characteristics of the sensor. It was found that the PVDF sensor could be applied to rapid measurement of the diagnostic level acoustic power.

Although the PVDF sensor shows a good potential in acoustic power measurement, the transformation mechanism between the acoustic and pyroelectric signals has not been particularly studied until now. In this paper, a physical model was introduced for a theoretical study of the pyroelectric effect under the excitation of ultrasound. Based on this model, a simulation program was built up by finite-element analysis method for analyzing the transformation mechanism, as well as for prediction of the waveform and amplitude of the generated pyroelectric signal. Furthermore, PVDF pyroelectric sensors were fabricated by using a damping composite backing material. The output pyroelectric signals were measured by a system with an ultra-

[1] The article is published in the original.

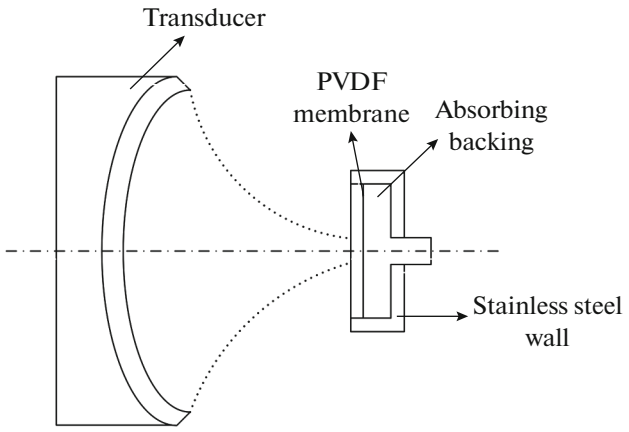

Fig. 1. Schematic of the PVDF pyroelectric sensor.

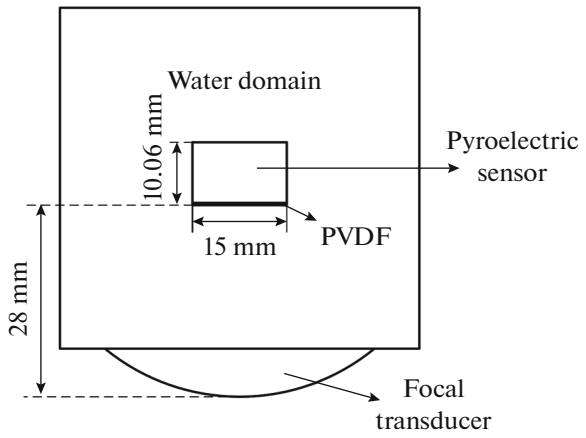

Fig. 2. Physical model.

sound focusing transducer. Then, the obtained results were compared with the simulation ones. Finally, it was confirmed that the physical model is suitable for analyzing pyroelectric characteristics and simulation of the output pyroelectric signal of the PVDF sensors. It can provide useful suggestions for the design and fabrication of the high sensitivity PVDF sensors for accurate acoustic measurement.

THEORETICAL ANALYSIS AND SIMULATION

Figure 1 represents a schematic plan of the PVDF pyroelectric sensor. The structure of the novel PVDF pyroelectric sensor is similar to the traditional piezoelectric transducer [8]. The difference is that this PVDF film is used as the pyroelectric element, which is backed by a high-damping composite backing material. For acoustic power measurements, an ultrasound focusing transducer is sited in front of the PVDF pyroelectric sensor as an acoustic source. Then the ultrasound wave can act on the surface of the sensor through the medium (ID water). Due to the impedance matching among water, PVDF and backing material, the most of the acoustic wave could propagate into the backing material. The acoustic attenuation of the backing material is so high that all the acoustic energy is absorbed and transformed into heat energy. Hence, there will be a temperature rise at the interface of PVDF and backing. Then, a pyroelectric signal is generated. The existing research shows that the rate of temperature rising and the amplitude of pyroelectric signal are proportional to the acoustic intensity [9].

According to the working process in Fig. 1, a physical model is built in a finite-element analysis software, as shown in Fig. 2. The focusing transducer has 28 mm focal length, 38 mm aperture and works at 1.27 MHz frequency. The PVDF pyroelectric sensor is 28 mm distance from the transducer. It has 15 mm diameter and 7 mm thickness. Both the sensor and transducer are immersed in water. The physical parameters of the PVDF and backing material are list in the Table 1.

A. Radiation Acoustic Field Characteristics

Before study the energy transformation in the PVDF pyroelectric sensor, it is necessary to know distribution characteristics of the acoustic field. Here, the acoustic field could be calculated by solving the wave equation in form of Helmholtz equation in 2D axisymmetric cylindrical coordinates [10, 11]:

$$\frac{\partial}{\partial r}\left[-\frac{r}{\rho_c}\left(\frac{\partial p}{\partial r}\right)\right]+r\frac{\partial}{\partial z}\left[-\frac{1}{\rho_c}\left(\frac{\partial p}{\partial z}\right)\right]-\left(\frac{\omega}{c_c}\right)^2\frac{rp}{\rho_c}=0, \quad (1)$$

where r and z are the radial and axial coordinates, p is the acoustic pressure, and ω is the angular frequency. The density ρ_c and sound velocity c_c are complex-valued to account for the material's damping properties. In the Eq. (1) it is assumed that ultrasound propagation is linear because the power of acoustic wave is not very high.

Based on the physical model as shown in Fig. 2, the acoustic pressure is simulated by using Eq. (1). The simulated ultrasound pressure distribution is shown in Fig. 3a. It could be found that the ultrasonic wave propagates through water and into the sensor. The wave is converged into a focal area, which is near the surface of the sensor. Further, it can be seen that the acoustic wave is absorbed by backing in a short depth, and the focal area shows a distortion. In order to know how the acoustic wave propagate in the sensor, the acoustic pressure amplitude profile along the acoustic axis (z-axis, $r = 0$) is shown in Fig. 3b. The maximum value of the acoustic pressure appears from $z = 22$ to 25 mm and is absorbed in a backing material of 3 millimeter ($z =$ 28 mm), which is close to the membrane. It is assumed that the conversion rate between the heat and acoustic energy is 100%. For accurate measurements of the ultrasonic power, the backing layer should be more

Table 1. Physical parameters of the PVDF and backing material

Material	Parameter	Value	Unit
PVDF	Thickness (d)	52	μm
	Density (ρ)	1780	kg/m^3
	Longitudinal Velocity (c_{PVDF})	2300	m/s
	Pyroelectric coefficient (p_c)	0.4×10^{-8}	C/cm^2 K
Backing material*	Density ($\rho_{backing}$)	1910	kg/m^3
	Longitudinal Velocity ($c_{backing}$)	1000	m/s
	Attenuation coefficient ($\alpha_{backing}$)	760	Np/m · MHz

* Backing material: a composite material is the polyurethane rubber filled with small micro-balloons, which can be purchased in National Physical Laboratory, UK)

than 3 mm thick, so that all the acoustic waves are absorbed.

B. Acoustic Absorption and Temperature Rise

The absorption of ultrasound energy will be translated into heat energy, which will directly cause a temperature rise in the backing material. To study the process of this transformation, a thermal module is coupled into the acoustic module, which was introduced in sub-section *A*. The rate of temperature rise could be described by the Biot's heat transfer equation, as shown in the following:

$$\dot{T} = \nabla(k\nabla T) + \frac{q_V}{c_V}, \qquad (2)$$

where $\dot{T}$ is the rate of temperature with respect to time, k is the thermal diffusivity, c_V is the volume specific heat and $\nabla = (\partial/\partial x)\mathbf{i} + (\partial/\partial y)\mathbf{j} + (\partial/\partial z)\mathbf{k}$, where **i, j, k** are unit vectors in the x, y, z directions, respectively.

q_V is the rate of heat production per unit volume. In this model, q_V represents the unit volume heat of the inside of sensor (PVDF and back material). However, due to the low attenuation coefficient of the water and the brief ultrasonic radiation, it is assumed that the heat diffused into the water can be ignored. q_V could be obtained by considering the divergence of the acoustic intensity vector [12]:

$$q_V = -\nabla\cdot\mathbf{I} = -\frac{\partial \mathbf{I}_x}{\partial x} = 2\alpha_{backing}(\mathbf{I}_{incident} - \mathbf{I}_{reflected}), \qquad (3)$$

where $\alpha_{backing}$ is the attenuation coefficient in the backing material, $\mathbf{I}_{incident}$ is the incident acoustic intensity component, $\mathbf{I}_{reflected}$ is the reflected acoustic inten-

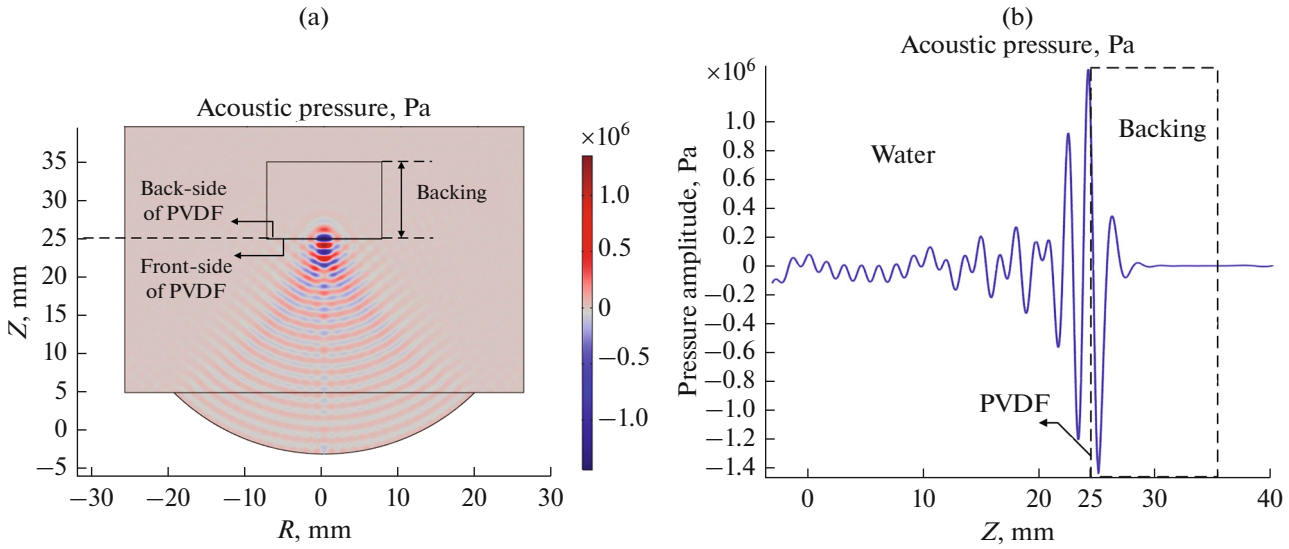

Fig. 3. Acoustic pressure distribution: (a) the acoustic pressure field in the water and the sensor, (b) acoustic pressure amplitude profile along the acoustic axis ($r = 0$).

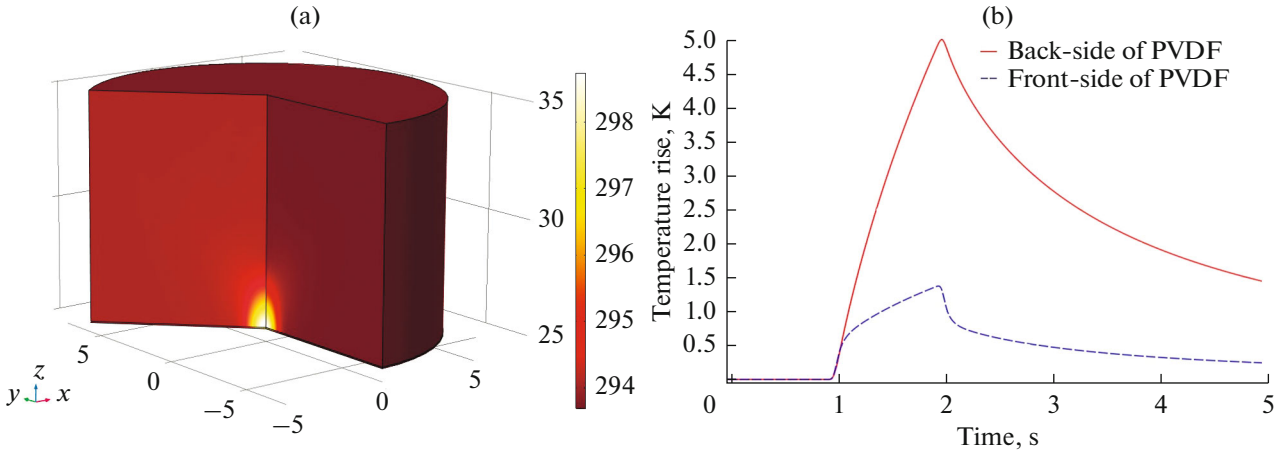

Fig. 4. Temperature change in the PVDF sensor: (a) temperature rise in the sensor, (b) temperature change at the front-side and back-side of PVDF.

sity component, and $\mathbf{I}_x$ is the axial component of the acoustic intensity vector.

Due to the heat conduction, there will be a temperature change in the PVDF membrane. The quantity $\Delta T(t)$ is introduced to represent the temperature elevation above ambient level [13].

$$\Delta T(t) = \frac{1}{2K}\int_0^{\xi}\int_0^{\frac{d}{2}} \frac{q_V(z)}{r(z)}\operatorname{erfc}\left(\frac{r}{\sqrt{4kt}}\right)xdxdz, \qquad (4)$$

where K is the thermal conductivity and ξ is the thickness of the heat source, d is the diameter of the heat source and r is the distance from the source.

By using the Eq. (2)–(4), the temperature distribution in the PVDF sensor is simulated. When the ultrasound transducer works during one second, the simulation result of the temperature rise in the PVDF sensor is shown in Fig. 4a. The oval-shaped heat spot has almost the same size as that of the acoustic absorption area shown in Fig. 3. At that, the maximum temperature rise is about five degrees on the membrane. Figure 4b shows the temperature change with time during the process of the ultrasonic radiation. The temperature difference at the front-side and back-side of PVDF with the same insonation is clearly demonstrated. This is due to the diffusion of the backing material heat into the PVDF and adjacent water. And the front-side temperature of PVDF is only 1 K higher than the ambient temperature. It is indicated that most of heat was absorbed by PVDF, and the diffusion of heat to adjacent water can be neglected. With the increase of ultrasonic radiation time, the accumulation of heat occurs continuously and through heat conduction leads to temperature rise on both sides of PVDF. Due to the thermal diffusion, the temperature will back down and the rate of temperature rise will drop quickly at initiation when the ultrasound transducer is switched off.

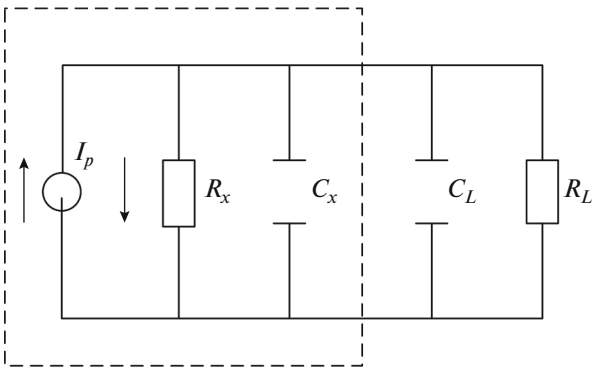

Fig. 5. Pyroelectric measurement equivalent circuit of the sensor.

As shown in Fig. 4b, there will be a temperature rise with respect to time. Due to the pyroelectric effect of the PVDF film, a pyroelectric signal will be generated. In the process of thermoelectric conversion, the PVDF could be considered as a current source, a capacitor and resistor in parallel [14]. This is shown in Fig. 5.

The dash frame is the equivalent circuit of pyroelectric PVDF film. C_L is the load capacitance, R_L is the load resistance. This circuit could be described in terms of the following differential equation:

$$\frac{p_e S}{C}\frac{d\Delta T}{dt} = \frac{U}{R_{\text{eq}}C} + \frac{dU}{dt}, \qquad (5)$$

where C is the capacitance of the layer of PVDF, I_p is the electrical current, p_e is the pyroelectric charge coefficient and S is the sensor surface area, $d\Delta T/dt$ is the rate of temperature rise with respect to time. R_{eq} is the parallel combination of R_x and R_L, R_x is the internal electrical resistance of sensor. U is the voltage at the input stage of the amplifier.

The pyroelectric signal generated by a transducer excited with ultrasound is simulated according to the theoretical analysis. Figure 6 shows the waveform of the pyroelectric signal, the ultrasound is acting on the PVDF sensor for 1 s. During the first several milliseconds (200 ms), the pyroelectric voltage increases rapidly to the maximum. This is due to the quick temperature increase and electric charge accumulation on the surface of the PVDF. When the ultrasound goes on acting on the sensor, the increase of the temperature will become slow and the pyroelectric signal will become small. If the transducer is switched off, there will be no energy support, and the temperature will decrease due to the cooling of the medium. Then, the electric charge will move in the opposite direction and there will be a significant decrease of the signal. Finally, the membrane reaches thermal equilibrium and returns to the neutral state. In theory, U_{on} (the output voltage of the sensor when it reaches a maximum during the switch-ON period) becomes approximately equal to U_{off} (the voltage of the sensor when it reaches a minimum during the switch-OFF period). They both can serve as parameters for measuring the delivered acoustic power.

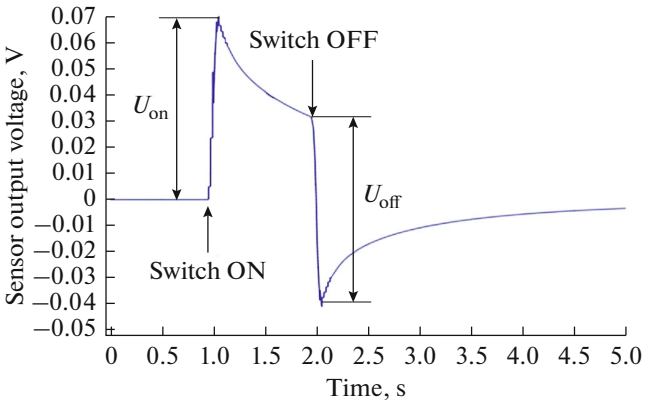

Fig. 6. Pyroelectric output voltage.

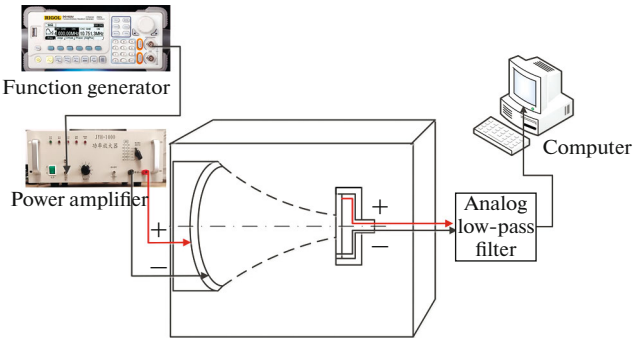

Fig. 7. Block diagram of the experimental setup.

EXPERIMENT AND MEASUREMENT

For the experimental study, a PVDF pyroelectric sensor was designed and fabricated. The structure of sensor is shown in Fig. 1. A 52 μm thickness PVDF film, with silver electrodes on both sides, was used as the active element. The backing material is provided by the National Physical Laboratory, UK, the material parameters are shown in Table 1. The front surface of the sensor was protected by a very thin epoxy layer for insulation from the water. Finally, the sensor was housed in a steel case and connected with cable and BNC connector.

For acoustic power measurement, an experimental system was built, as shown in Fig. 7. A spherical focusing ultrasound transducer was excited by a function generator (RIGOL DG1022U) and power amplifier (JYH-1000). Due to the piezoelectricity of the PVDF film, an analog low-pass filter was connected with the PVDF sensor for acquisition of the pure pyroelectric signals. A computer was used for date acquisition, storage and final processing.

When a 135 mW focal acoustic power was used, the pyroelectric output signals were acquired and stored by the system. By changing the time of duration of the acoustic wave (ΔT = 0.1, 2.1, 4.2 s), different pyroelectric output signals were acquired, as shown in Fig. 8a. At ΔT = 0.1 s, the signal shows the shape similar to that of the shock wave. Besides that, the waveform of the pyroelectric signals was typical, as simulated by the physical model introduced in section 2. For ΔT = 2 and ΔT = 4 s, the simulated results are shown in Fig. 8b. However, there are some subtle differences in the amplitude. The one reason of this difference is the thermal dispersion. The adiabatic environment is taken into theoretical calculation, but the sensor is immersed in water. A temperature change would be existing on the interface in experimental measurements. Another reason is the reflection of sound wave on the surface of sensor during the process of measuring. Moreover, in practice, measured values U_{on} and U_{off} may differ due to the effect of convection, streaming at the boundary between the sensor and the water coupling medium, and other confounding phenomena.

From Fig. 8, it is found that the PVDF sensor has a quick thermal response capacity of the ultrasound. At that, the U_{on} time of the sensor is no more than 0.1 s. To further know the U_{on} time of the transducer, an experiment was established, which is the $\underline{U}_{on}$ with different radiation time of the transducer. The results are summarized in Fig. 9. On the premise of the same ultrasound radiation power, when the radiation time of transducer is less than 130 milliseconds, U_{on} is proportional to time. With the increase of irradiation time, U_{on} tends to change slowly and the maximum first appears at 320 ms and finally does not change with time. Hence, it can be one of the parameters to evaluate the acoustic power. Compared with the mea-

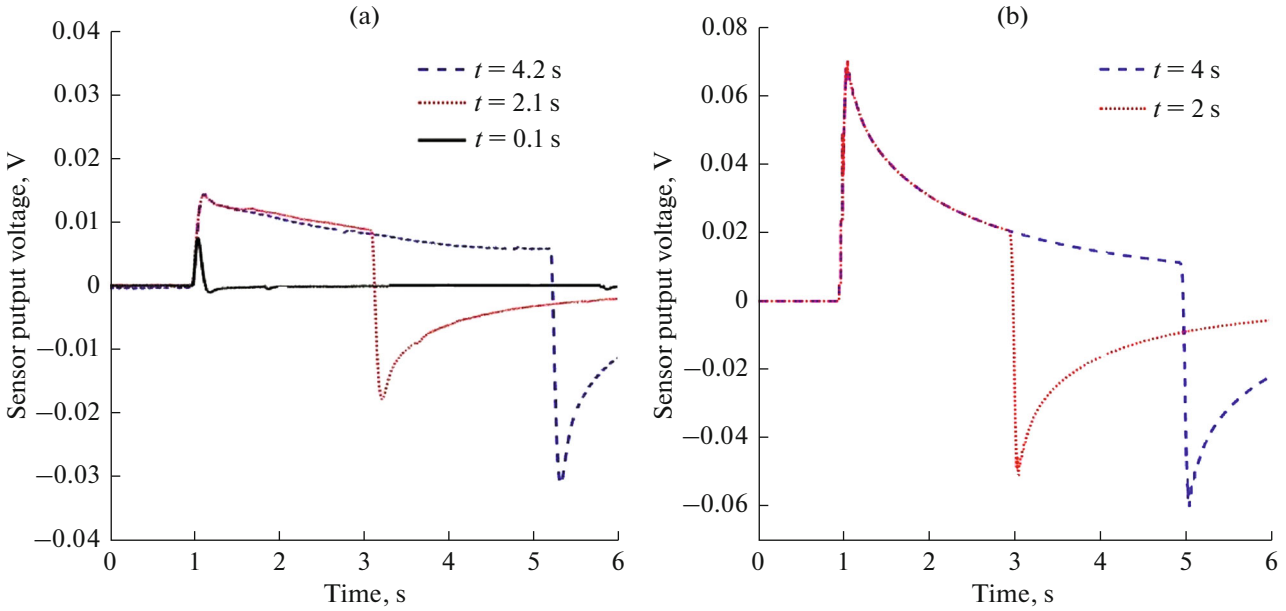

Fig. 8. Pyroelectric output signals: (a) output signal by experiment, (b) output signals by simulation results.

surement of calorimetry [15], the time of thermal response was quicker, since it did not need thermal equilibrium to be reached.

CONCLUSIONS

In this paper, a physical model was built up for study of the mechanism of energy transformation between ultrasound and pyroelectric signals. To calculate and analyze the acoustic field and temperature distribution at the same time, a simulation program was established by using a finite-element analysis software. The simulation results show how the ultrasound wave transforms into heat and causes the temperature increase in both backing material and PVDF film. It was found that the heating rate determines the waveform of the pyroelectric signal. Besides that, a PVDF pyroelectric sensor was fabricated and used for acoustic power measurements. The experimental results demonstrated the effectiveness of the physical model. According to the analysis, it was found that the pyroelectric PVDF sensor could output the pyroelectric signal as soon as the ultrasound acts on the sensor. In addition, the duration of the signal is almost the same as the loading time of the ultrasound signal. The amplitude of the pyroelectric signal is proportional to the acoustic power.

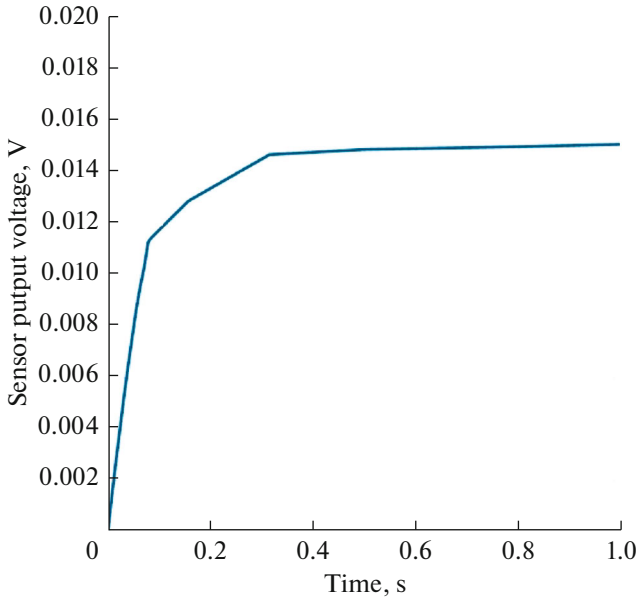

Fig. 9. Variation of U_{on} with different radiation time.

According to the theory and experimental study, the novel application of the PVDF pyroelectric sensor in acoustic power measuring is proven. After further optimization of the physical model, more useful suggestions for the design and fabrication of the high sensitivity PVDF sensor can be provided, to achieve highly accurate measurements of ultrasonic power. The novel sensor can be used for rapid power detection of ultrasonic medical equipment after metrological calibration.

ACKNOWLEDGMENTS

The authors gratefully acknowledge the financial support of The National Key Research and Development Program of China (Project no. 2016YFF0201006), The National Natural Science Fund of China (Project

no. 11474259, 81471664), Zhejiang province natural science foundation of China (Project number: LY15E050012).

REFERENCES

1. R. W. Whatmore, Rep. Prog. Phys. **49** (49), 1335 (1986).
2. Xiaopei Guo, *Preparation of PVDF Thin Lm and Measurement of Pyroelectric Unit Detector* (Univ. of Electronic Science and Technology of China, Chengdu, 2015).
3. Fang Wang, Wen chao Han, Huanhuan Li, and Yufeng Peng, J. Funct. Mater. Devices **18** (5), 387 (2012).
4. Menglu Wang and Lei Zhang, Exp. Sci. Technol. **15** (1), 29 (2017).
5. I. M. Margulis and M. A. Margulis, Acoust. Phys. **51** (6), 695 (2005).
6. B. Zeqiri, P. N. Gelat, J. Barrie, and C. J. Bickley, IEEE Trans. Ultrason., Ferroelectr. Freq. Control **54** (11), 2318 (2007).
7. B. Zeqiri, A. Shaw, P. N. Gélat, D. Bell, and Y. C. Sutton, J. Phys.: Conf. Ser. **1**, 105 (2004).
8. L. N. Magdich, V. I. Balakshy, and S. N. Mantsevich, Acoust. Phys. **63** (6), 645 (2017).
9. K. Beissner, in *Ultrasonic Exposimetry*, Ed. by M. C. Ziskin and P. A. Lewin (CRC Press, Boca Raton, FL, 1993), p. 163.
10. Ge Pu Guo, Hui Dan Su, He Ping Ding, and Qing Yu Ma, Acta Phys. Sin–Chin. Ed. **66** (16), 164301 (2017).
11. O. D. Rumyantseva and A. S. Shurup, Acoust. Phys. **63** (1), 95 (2017).
12. M. R. Bailey, V. A. Khokhlova, O. A. Sapozhnikov, S. G. Kargl, and L. A. Crum, Acoust. Phys. **49** (4), 369 (2003).
13. W. L. Nyborg, Phys. Med. Biol. **33** (7), 785 (1988).
14. Min Wei, *Study on Measuring System of Pyroelectric Material under DC-Biased Electric Field* (HuangZhong Univ. of Science and Technology, 2012).
15. A. Shaw, Ultrasound Med. Biol. **34** (8), 1327 (2008).